R. & M. No. 3125

MINISTRY OF AVIATION

AERONAUTICAL RESEARCH COUNCIL
REPORTS AND MEMORANDA

Vectorial Analysis of Flight Flutter Test Results

By E. G. Broadbent and E. Violet Hartley

LONDON: HER MAJESTY'S STATIONERY OFFICE
1961
PRICE: 9*s*. 6*d*. NET

Vectorial Analysis of Flight Flutter Test Results

By E. G. Broadbent and E. Violet Hartley

Communicated by the Director-General of Scientific Research (Air)

Ministry of Supply

*Reports and Memoranda No. 3125**

February, 1958

Summary. A binary flexure-torsion analysis has been made to check theoretically a method for the prediction of flutter which depends on plotting vectorially the amplitudes of response relative to the exciting force and extracting the relevant damping rate. The results of this calculation are given in the form of graphs both of the vector plots themselves and of the estimated damping rate against forward speed. The estimated damping rates are compared with calculated values. The method has the advantage that, in a flight flutter test, damping can be estimated from continuous excitation records; the method is an extension of the Kennedy and Pancu technique used in ground resonance testing.

1. *Introduction.* The measurement of normal modes in a ground resonance test needs an elaborate technique both to ensure that the modes are reasonably orthogonal, and to ensure that no mode is missed. The presence of structural damping presents one of the main difficulties. Kennedy and Pancu[1] have suggested a method of analysing the recordings taken by plotting vectorially the displacements relative to the exciting force. Near circles are obtained for each resonance and practical experience seems to show that this type of plot considerably reduces the likelihood of missing a resonance and also improves the accuracy of determining the resonant frequency. This in itself leads to modes being measured which are a better approximation to the true normal modes than is usually possible from amplitude plots alone. In addition, the structural damping can be estimated directly for each resonance.

Because of its success in ground resonance tests the idea has arisen of adapting the technique for flight flutter testing. It is hoped that from the flight test under continuous excitation the resonances might be obtained in the same way as from a ground test, with at the same time estimates of the overall damping at each resonance frequency. Thus a graph of damping rate against air-speed can be obtained from a continuous excitation method of flight flutter testing. In this way it is hoped to obtain the best of two worlds; continuous excitation allows more accurate analysis in the presence of buffeting than is possible from a decaying oscillation, and at the same time damping can be plotted against air speed; and damping gives a more reliable warning of the approach to flutter than does amplitude response. Near the flutter speed, however, the analysis has to deal with a different type of equilibrium than in a ground resonance test, because the aerodynamic forces are powerful and do not represent a conservative system. In order to see whether this leads to any difficulty in application, a simple flexure-torsion binary example has been worked out in the present paper and analysed by

* R.A.E. Tech. Note Struct. 233, received 18th February, 1958.

the Kennedy-Pancu method at various forward speeds up to the flutter speed. The dampings are obtained and plotted against air-speed and the results are found to agree well with calculated dampings. This promises well for the method but, of course, the vastly greater complications to be found in reality can be expected to lead to a more confused picture than that obtained from a binary example.

2. *Theory of the Method.* The basis of the theory is outlined here for convenience.

2.1. *One Degree of Freedom.* The equation of motion for one degree of freedom can be written in the form:

$$a\ddot{q} + e(1 + ig)q = Fe^{i\omega t} \tag{1}$$

for a generalised exciting force $Fe^{i\omega t}$, where a is an inertia coefficient, e is an elastic coefficient, q is a generalised co-ordinate and g is the phase angle of the restoring force (the damping coefficient). The steady solution will be motion of the form $e^{i\omega t}$, so we substitute $q = \bar{q}e^{i\omega t}$.

Equation (1) now becomes:

$$[-\omega^2 a + e(1 + ig)]\,\bar{q} = F\,. \tag{2}$$

We let ω_0 be the natural frequency of the one degree of freedom, i.e., $\omega_0{}^2 = e/a$ and we obtain:

$$a\,[\omega_0{}^2(1 - \tilde{\omega}^2) + ig\omega_0{}^2]\,\bar{q} = F\,, \tag{3}$$

where $\tilde{\omega}^2 = (\omega/\omega_0)^2$.

For the purpose of vector plotting $\bar{q}$ is written in the form:

$$\bar{q} = q_r + iq_i\,. \tag{4}$$

For any exciting frequency, ω, the quantities q_r and q_i can now be calculated and plotted on an Argand diagram to give the response vector at that frequency relative to the exciting force, i.e., F is taken to lie along the real axis.

Substituting equation (4) in equation (3) and equating real and imaginary parts leads to:

$$a\omega_0{}^2\,[q_r(1 - \tilde{\omega}^2) - q_i g] = F \tag{5}$$

and

$$a\omega_0{}^2\,[q_r g + q_i(1 - \tilde{\omega}^2)] = 0\,. \tag{6}$$

Hence

$$q_r = \frac{F}{a\omega_0{}^2}\left[\frac{1 - \tilde{\omega}^2}{(1 - \tilde{\omega}^2)^2 + g^2}\right] \tag{7}$$

and

$$q_i = \frac{F}{a\omega_0{}^2}\left[\frac{-g}{(1 - \tilde{\omega}^2)^2 + g^2}\right]. \tag{8}$$

As ω is varied the locus of points (q_r, q_i) is a smooth curve obtained by eliminating $\tilde{\omega}$ from these two equations:

$$\frac{q_r{}^2}{q_i{}^2} = -\frac{F}{a\omega_0{}^2 q_i g} + 1 \tag{9}$$

or

$$q_r{}^2 + q_i{}^2 + \left(\frac{F}{a\omega_0{}^2 g}\right) q_i = 0\,. \tag{10}$$

This is the equation of a circle with its diameter lying on the negative imaginary axis and passing through the origin (*see* Fig. 1).

The position of resonance.

Resonance occurs when $\tilde{\omega} = 1$ and from equation (7) $q_r = 0$, i.e., the vector OC on Fig. 1 represents the amplitude at resonance. We can obtain a relation between the rate of change of frequency along the curve at resonance and the damping g, so that if the curve itself is obtained from measurements on a structure of unknown damping, the damping can be estimated.

Consider the point D in Fig. 1 when the frequency is $\omega_0 + \delta\omega$. At D

$$\frac{q_r}{q_i} = \tan\frac{\theta}{2} \tag{11}$$

$$= \frac{1 - \tilde{\omega}_D^2}{-g}, \tag{12}$$

from equations (7) and (8).

Hence

$$g = \frac{\delta\omega}{\omega_0}\left(2 + \frac{\delta\omega}{\omega_0}\right)\cot\frac{\theta}{2}. \tag{13}$$

It can be seen from equation (13) that if $\delta\omega/\omega_0$ is small, equal angles will be subtended by equal frequency increments on either side of the resonance. In the particular case when $\theta = \frac{1}{2}\pi$ we have:

$$\left.\begin{aligned} \tilde{\omega}_A^2 &= 1 + g = \left(\frac{\omega_A}{\omega_0}\right)^2 \\ \text{and when } \theta = -\tfrac{1}{2}\pi \quad \tilde{\omega}_B^2 &= 1 - g = \left(\frac{\omega_B}{\omega_0}\right)^2 \end{aligned}\right\}. \tag{14}$$

Hence

$$\left.\begin{aligned} 2g &= \frac{\omega_A^2 - \omega_B^2}{\omega_0^2} \\ \text{and} \quad 2 &= \frac{\omega_A^2 + \omega_B^2}{\omega_0^2} \end{aligned}\right\}. \tag{15}$$

Whence

$$g = \frac{\omega_A^2 - \omega_B^2}{\omega_A^2 + \omega_B^2} \tag{16}$$

$$\approx \frac{(\omega_A - \omega_B)}{\omega_0}.$$

It is common practice in this country to express the damping as a percentage of the critical damping. As long as the damping is small, g can be directly related to the percentage of critical damping which is derived from the concept of velocity damping, *i.e.*, the appropriate differential equation is:

$$a\ddot{q} + d\dot{q} + eq = Fe^{i\omega t}. \tag{17}$$

Comparing this with equation (1)

$$d\dot{q} = eigq \tag{18}$$

and substituting $q = \bar{q}e^{i\omega t}$,

$$i\omega d = ieg. \tag{19}$$

Hence

$$g = \frac{\omega d}{e}. \tag{20}$$

But $d = (2c/c_c)\sqrt{(ae)}$ where c/c_c is the fraction of critical damping.

Hence

$$g = 2\frac{\omega}{\omega_0}\left(\frac{c}{c_c}\right), \tag{21}$$

so that at resonance

$$g = 2\frac{c}{c_c} = \frac{d}{\sqrt{(ae)}}. \tag{22}$$

It should be noted that if the damping is of the form given by equation (17), the locus of points (q_r, q_i) is no longer a circle; the steady solution will be motion of the form $e^{i\omega t}$, and substituting $q = \bar{q}e^{i\omega t}$ the equation becomes:

$$(-a\omega^2 + di\omega + e)\bar{q} = F. \tag{23}$$

Proceeding as before we obtain:

$$q_r = \frac{F}{a{\omega_0}^2}\frac{1 - \tilde{\omega}^2}{(1 - \tilde{\omega}^2)^2 + \tilde{\omega}^2\bar{g}^2} \tag{24}$$

and

$$q_i = \frac{-F}{a{\omega_0}^2}\left[\frac{\tilde{\omega}\bar{g}}{(1 - \tilde{\omega}^2)^2 + \omega^2\bar{g}^2}\right]. \tag{25}$$

Here $\bar{g} = d/\sqrt{(ae)}$, so that the two systems represented by equations (1) and (23) will have the same properties at resonance if $g = \bar{g}$. The vector q defined by equations (24) and (25) now describes a quartic curve starting at the point $(F/(a{\omega_0}^2), 0)$ when $\omega = 0$ and finishing at the origin when $\omega \to \infty$; any other branches are for unreal frequencies. In practice, for small values of $\bar{g}$ the curve is indistinguishable from a circle except at low frequencies; this is shown in Fig. 2 where the circle of equations (7) and (8) is compared with the quartic of equations (24) and (25).

2.2. *Two Degrees of Freedom.* Kennedy and Pancu[1] suggest that with N degrees of freedom there will be N near circles. For any particular resonance, the best circle is put through the points and the resonance is given by the minimum $\delta\omega/\delta s$, where s represents distance along the curve. If equal increments of ω are taken, the greatest change of phase gives the resonance. The damping (g) can then be extracted as for one degree of freedom.

Because this method appears to be the best way of estimating damping in ground resonance tests, it has been suggested that it might well be extended to the estimation of damping in a flight flutter test, where continuous excitation is being employed. The method may be difficult when the dampings are high at medium flight speeds, but should improve again for low damping near the flutter speed. The difference between the flight condition near the flutter speed and the ground condition, where the damping is low in each case, is that in flight there will be large asymmetric couplings arising from the aerodynamic forces. It was decided to see how important these were in practice by calculating the response of a simple binary example at various speeds up to the flutter speed.

3. *Binary Example.* 3.1. *Basic Data.*

Geometry.

For simplicity a two-dimensional rigid wing, restrained by springs in vertical translation and pitch, was considered. The two degrees of freedom are:

Vertical translation: $z = cq_1$ (representing wing flexure)

Pitch: $\alpha = q_2$ (representing wing torsion)

In general $z = cq_1 + xq_2$.

The axis of pitch is at the half-chord.

The axis of centre of gravity is at the half-chord.

Since the modes are uncoupled at zero flight speed they are normal modes and the frequency ratio is $\omega_z : \omega_\alpha :: 0{\cdot}4676 : 1$.

Structural damping at a value of $g = 0{\cdot}02$ is assumed to be present in each degree of freedom. It is assumed that displacements to be recorded in flight tests are linear displacements at the half-chord, quarter-chord and leading edge and the angle of pitch. Thus the first and last of these 'pick-ups' give measurements proportional to the generalised co-ordinates q_1 and q_2 respectively. Finally, it is assumed that the excitation is linear vertical excitation applied at the quarter-chord.

3.2. *Wing flutter.* The aerodynamic derivatives are assumed to be constant both with the frequency parameter and forward speed, *i.e.*, any Mach-number effect is neglected.

The equations for free oscillation can be written in the form:

$$\begin{bmatrix} -14{\cdot}04\nu^2 + 1{\cdot}96\nu v i & 0{\cdot}63\nu v i + 2{\cdot}27v^2 \\ +(1 + 0{\cdot}02i)y_0 & \\ & -0{\cdot}8906\nu^2 + 0{\cdot}24\nu v i - 0{\cdot}565v^2 \\ -0{\cdot}49\nu v i & +0{\cdot}29(1 + 0{\cdot}02i)y_0 \end{bmatrix} \begin{bmatrix} q_1 \\ q_2 \end{bmatrix} = 0, \qquad (26)$$

where V_c is the flutter speed, $\nu = \omega c/V_c$, $v = V/V_c$, $y_0 = E_{11}/(\rho V_c^2 sc^2)$, c is the wing chord, and s is the wing span. The equations were solved for y_0 with $v = 1$ (corresponding to the critical flutter speed), and gave $y_0 = 2{\cdot}92$ and $\nu = 0{\cdot}666$.

From a knowledge of y_0 it is possible to relate any known E_{11} (the spring restraint against vertical translation), to an actual flutter speed (V_c), knowing the dimensions. Here, however, we are only interested in the relative speeds, i.e., v, the fraction of V_c.

3.3. *Response Calculations.* With the excitation at the quarter-chord and after the substitution for $y_0 = 2{\cdot}92$, equation (26) becomes:

$$\begin{bmatrix} (-14{\cdot}04\nu^2 + 2{\cdot}92) + & 2{\cdot}27v^2 + 0{\cdot}63\nu v i \\ +(1{\cdot}96\nu v + 0{\cdot}0584)i & \\ & (-0{\cdot}8906\nu^2 - 0{\cdot}565v^2 + 0{\cdot}8468) + \\ -0{\cdot}49\nu v i & +(0{\cdot}24\nu v + 0{\cdot}016936)i \end{bmatrix} \begin{bmatrix} q_1 \\ q_2 \end{bmatrix} = \begin{bmatrix} 1 \\ -0{\cdot}25 \end{bmatrix} F, \qquad (27)$$

where F is an arbitrary force level. For simplicity F is taken to be unity in the calculation which follows. Values of $v = 0$, $0{\cdot}25$, $0{\cdot}5$, $0{\cdot}75$, $0{\cdot}9$ and $1{\cdot}0$ were chosen, and in each case q_1 and q_2 were calculated for a set of increments in ν. Assuming perfect accuracy of recording the measurements taken in flight from the four 'pick-ups' (half-chord, quarter-chord, leading edge, pitching angle) would be q_1, $q_1 - \frac{1}{4}q_2$, $q_1 - \frac{1}{2}q_2$, q_2. These are plotted vectorially in Figs. 3 to 26.

3.4. *Comments on Figures.* It is convenient to comment on the Figures briefly in groups for each forward speed. On the Figures, the displacements of the four 'pick-ups' (*see* above) are referred to as displacement 1, displacement 2, displacement 3, displacement 4, respectively.

$v = 0$.—Figs. 3 to 6.

Since the first and fourth 'pick-ups' measure the generalised co-ordinates q_1 and q_2, which are normal co-ordinates at zero speed, they each show a single perfect circle.

The second and third 'pick-ups' measure displacements which are dependent on both generalised co-ordinates and therefore show both resonances, with some slight distortion of the circles in each case. The two circles in each case lie on the same side of the real axis.

The resonance frequencies are given by $\nu = 0{\cdot}456$ and $0{\cdot}975$.

$v = 0{\cdot}25$.—Figs. 7 to 10.

The size of the circles has diminished considerably in each case. The effect of the couplings causes the circles to be less perfect; in the first and fourth cases a distorted circle is introduced.

The resonance frequencies are given by $\nu = 0{\cdot}455$ and $0{\cdot}955$.

$v = 0{\cdot}5$.—Figs. 11 to 14.

The size of the original circle from the first and fourth 'pick-ups' has again been decreased, but the introduced coupling near-circle has increased. Both circles, from each of the second and third 'pick-ups', have decreased in size.

The resonance frequencies are given by $\nu = 0{\cdot}46$ and $0{\cdot}895$, and the higher frequency is now reducing fairly rapidly as speed is increased.

$v = 0{\cdot}75$.—Figs. 15 to 18.

From the first 'pick-up' the original circle is still decreasing but the new circle is of truer form and its size is increasing. From the fourth 'pick-up' both circles are increasing in size. The size of both circles from each of the second and third 'pick-ups' is less.

The resonance frequencies are given by $\nu = 0{\cdot}4375$ and $0{\cdot}78$.

$v = 0{\cdot}9$.—Figs. 19 to 22.

The size of the original circle from the first 'pick-up' has again decreased, but the new circle has increased and is now greater than the original. From the fourth 'pick-up' the size of both circles is increasing, but there is no resonance obtainable from the lower-frequency circle. From the second 'pick-up', the size of the circle with the higher frequency has greatly increased, so that it is now almost equal to the lower-frequency circle. The circle with the higher frequency from the third 'pick-up' has increased in size, but both circles are more imperfect.

The resonance frequencies are given by $\nu = 0{\cdot}39$ and $0{\cdot}705$.

$v = 1{\cdot}0$.—Figs. 23 to 26.

As this is the flutter speed, one of the circles must now have increased indefinitely in size at the flutter frequency. This is in fact the circle corresponding to the higher frequency.

The response curves are all plotted on the same Figure to the same scale for each of the four 'pick-ups' (Figs. 27 to 30).

3.5. *Estimation of Damping in Flight and Conclusion.* As outlined in Section 2, we estimate the damping c/c_e from the circles. Near each resonance suitable equal increments in frequency are chosen, and these are marked on the curves of Figs. 3 to 26. The actual resonance is picked out from the Figures by using a pair of dividers to get the maximum phase change. In this example there was never any difficulty in putting a circle through the points (these circles are shown in Figs. 3 to 26) and the damping was estimated from convenient increments of frequency as can be seen from the construction on the Figures.

The damping as obtained from each 'pick-up' was then plotted against forward speed, and the results are shown in Fig. 31. Since our example is completely specified mathematically, the dampings can also be calculated exactly. In Fig. 32 the calculated roots are plotted and compared with the estimates from each of the four 'pick-ups'. Fig. 32a, shows the change in frequency of the lower frequency with forward speed and Fig. 32b shows the change in damping. Figs. 32c and d give the corresponding results for the higher-frequency root, which is the one that leads to flutter at $v = 1{\cdot}0$. The agreement in general between the different estimates and the calculated values is very good.

The only serious error in the lower-frequency root is obtained from the rotational 'pick-up'; this seems to give the wrong trend of frequency with speed when the damping exceeds 10 per cent of critical, a condition which would in any case be unimportant in practice. For the higher-frequency root the accuracy is good throughout, and best for this same rotational 'pick-up', as might be expected on qualitative grounds. Any of the 'pick-ups', however, would give a good prediction of the flutter speed (*see* Fig. 32d), provided the speed increments chosen were not too large.

From flight measurements in practice one could scarcely hope to get such a consistent set of results as has been obtained from the estimates in this simple binary example. On the other hand, the example does suggest that the method is sound in principle, so that if there are practical arguments which favour recording from continuous excitation rather than decaying oscillations, the Kennedy and Pancu type of analysis is likely to provide good results. It may well be, however, that with many degrees of freedom present, as on real aircraft, the choice of 'pick-up' position is more important than in the binary example. In general, the flight analysis would be carried out for two or three 'pick-ups' as a normal safety precaution.

LIST OF SYMBOLS

a		An inertia coefficient
d		A damping coefficient
e		An elastic coefficient
g		The phase angle of the restoring force (a damping coefficient)
q		A generalised co-ordinate
F		A generalised exciting force
ω_0		The natural frequency of one degree of freedom
ω		The exciting frequency
$\tilde{\omega}^2$	$=$	$\left(\frac{\omega}{\omega_0}\right)^2$
V_e		The flutter speed
V		The forward speed
v	$=$	V/V_e
ν		A frequency parameter $\omega c/V_e$
c		The wing chord; and also in the damping ratio c/c_e (*See* line under (20))
s		The wing span
ρ		The air density
E_{11}		The spring restraint against vertical translation
y_0	$=$	$\frac{E_{11}}{\rho V_e^2 sc^2}$
z		Vertical displacement
α		The angle of pitch

REFERENCE

No.	*Author*	*Title, etc.*
1	C. C. Kennedy and C. D. P. Pancu ..	Use of vectors in vibration measurement and analysis. *J. Ae. Sci.* Vol. 14. No. 11. November, 1947.

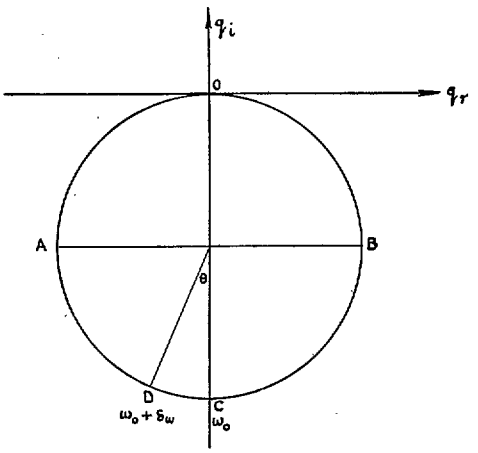

FIG. 1. Vector diagram for one degree of freedom—Hysteresis damping.

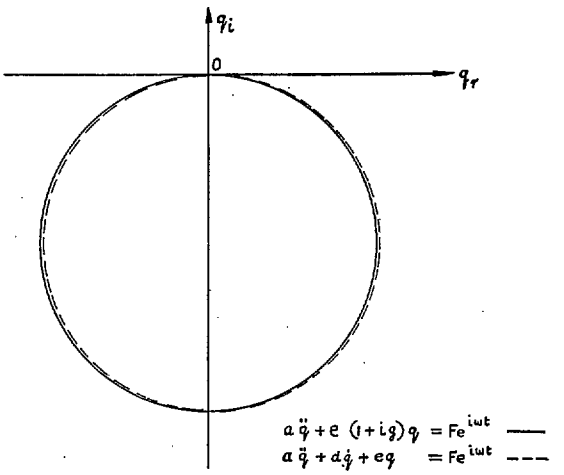

FIG. 2. Vector diagram for one degree of freedom—Comparison between hysteresis and velocity damping.

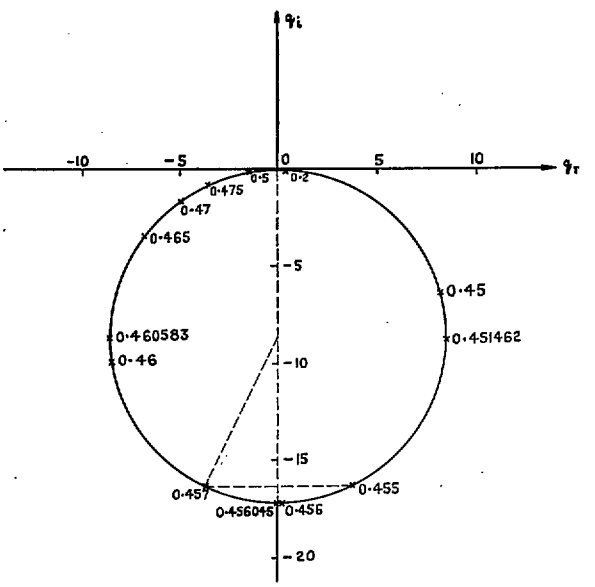

FIG. 3. Vector diagram for binary example: $v = 0$, displacement 1.

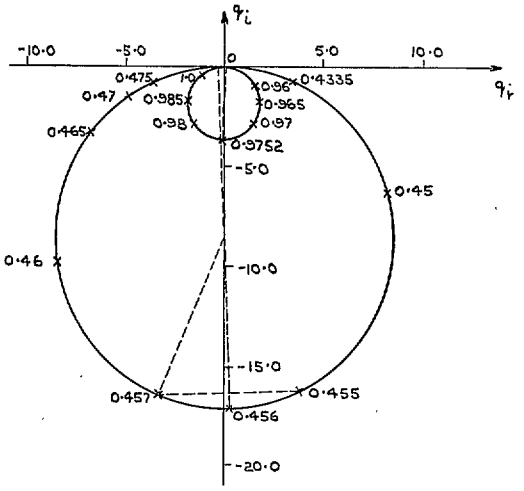

FIG. 4. Vector diagram for binary example: $v = 0$, displacement 2.

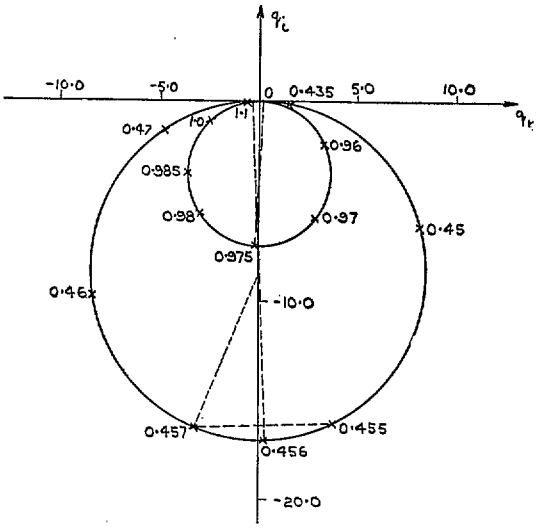

FIG. 5. Vector diagram for binary example: $v = 0$, displacement 3.

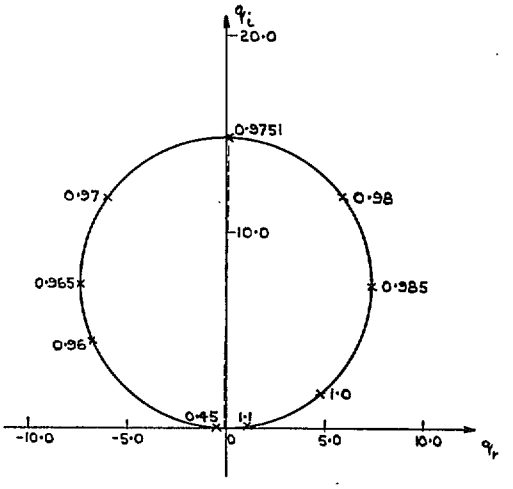

FIG. 6. Vector diagram for binary example: $v = 0$, displacement 4.

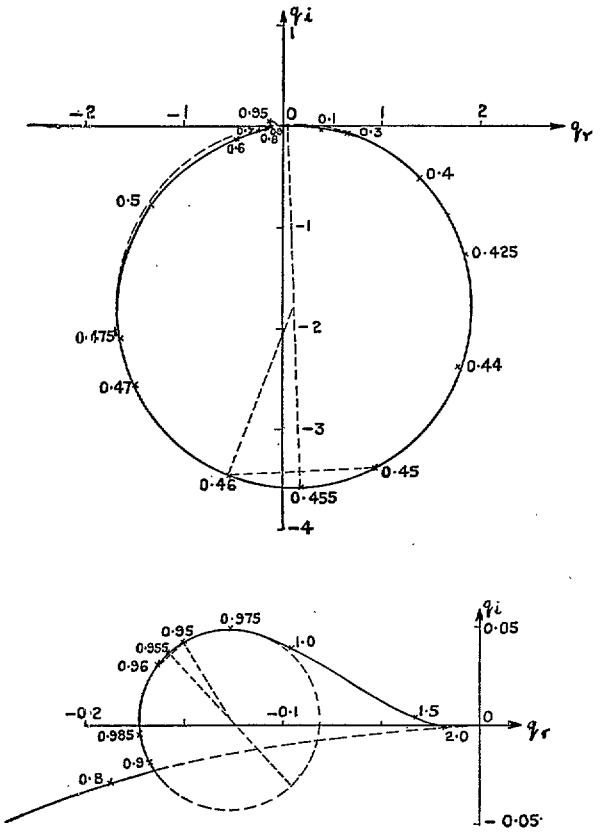

FIG. 7. Vector diagram for binary example: $v = 0{\cdot}25$, displacement 1 (Lower figure.—Detailed presentation of part of main figure).

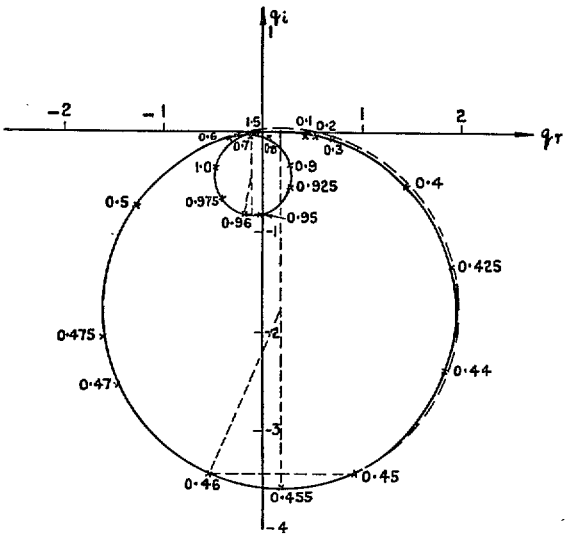

FIG. 8. Vector diagram for binary example: $v = 0{\cdot}25$, displacement 2.

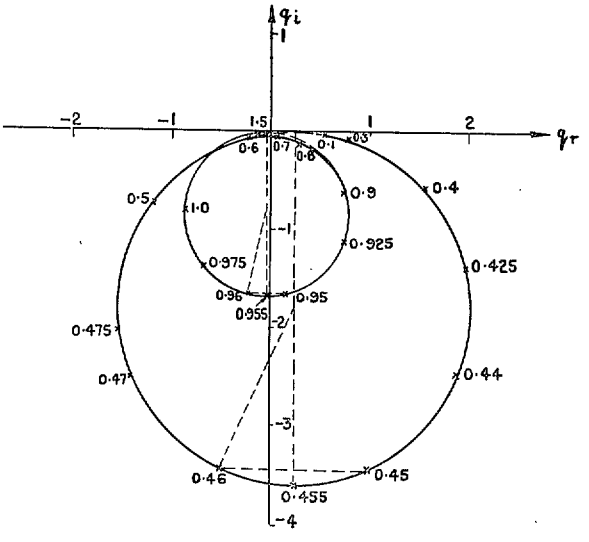

FIG. 9. Vector diagram for binary example: $v = 0{\cdot}25$, displacement 3.

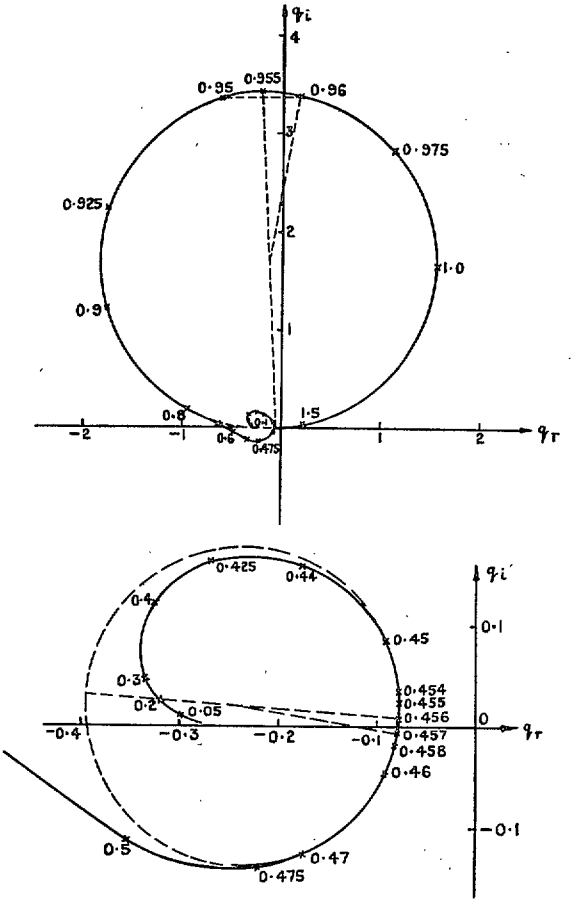

FIG. 10. Vector diagram for binary example: $v = 0{\cdot}25$, displacement 4 (Lower figure.—Detailed presentation of part of main figure).

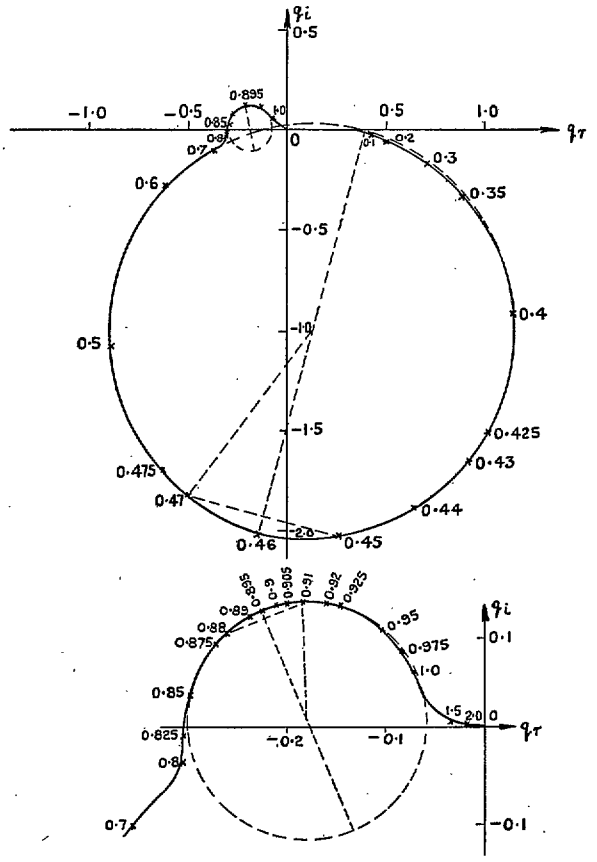

FIG. 11. Vector diagram for binary example: $v = 0{\cdot}5$, displacement 1 (Lower figure.—Detailed presentation of part of main figure).

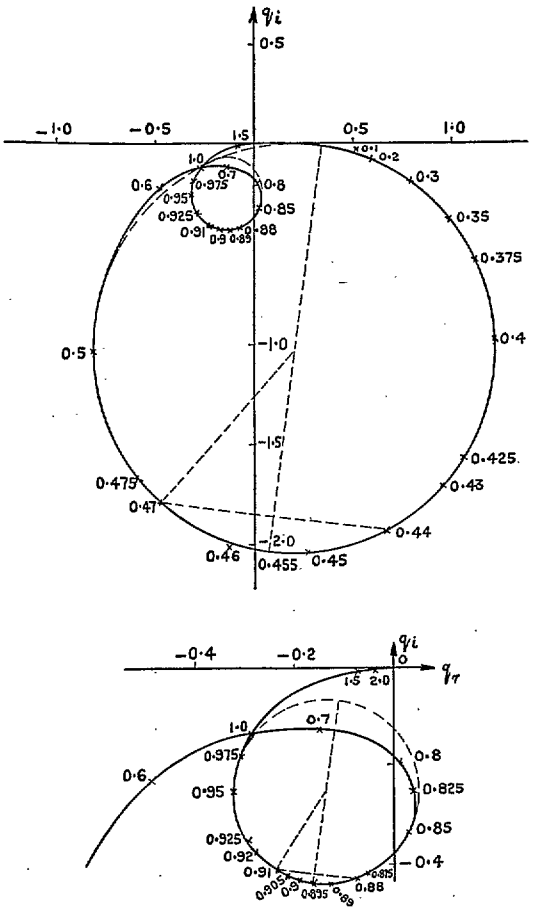

FIG. 12. Vector diagram for binary example: $v = 0{\cdot}5$, displacement 2 (Lower figure.—Detailed presentation of part of main figure).

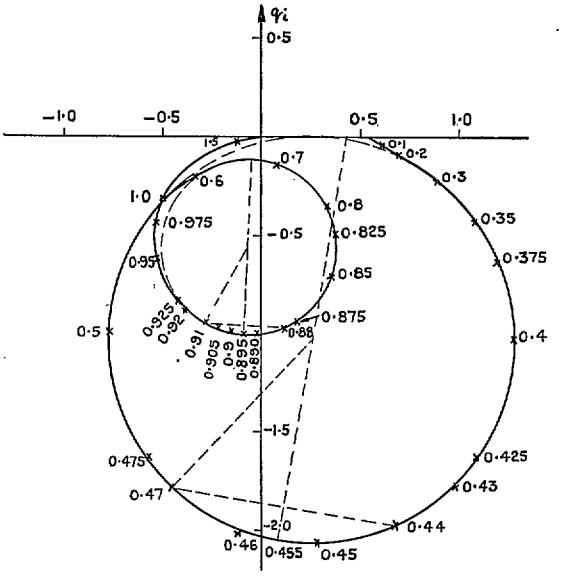

FIG. 13. Vector diagram for binary example: $v = 0 \cdot 5$, displacement 3.

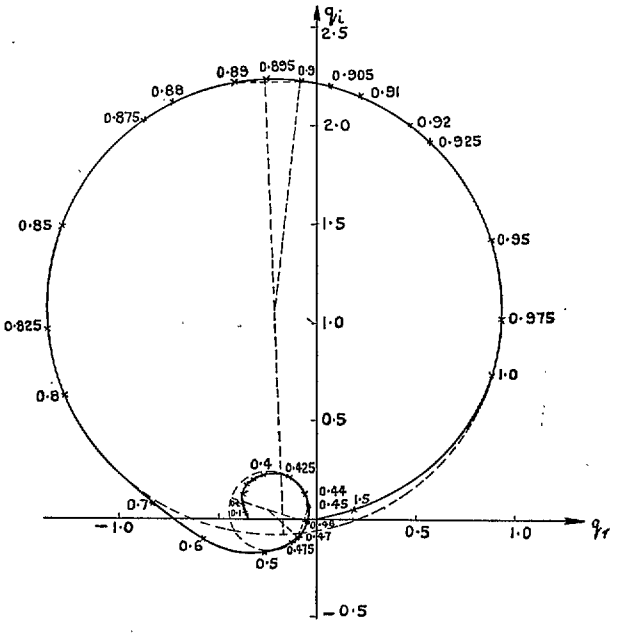

FIG. 14. Vector diagram for binary example: $v = 0 \cdot 5$, displacement 4.

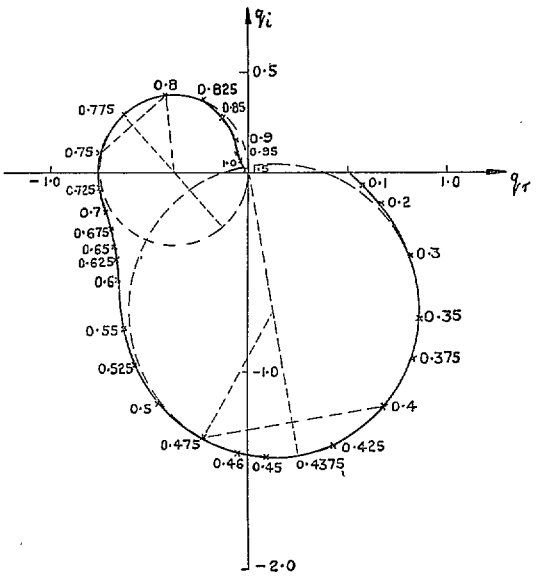

FIG. 15. Vector diagram for binary example: $v = 0{\cdot}75$, displacement 1.

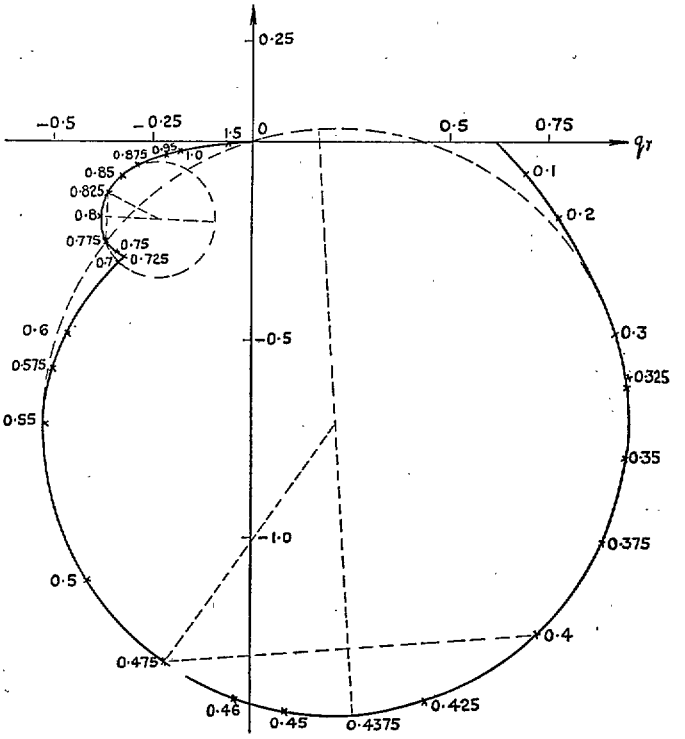

FIG. 16. Vector diagram for binary example: $v = 0{\cdot}75$, displacement 2.

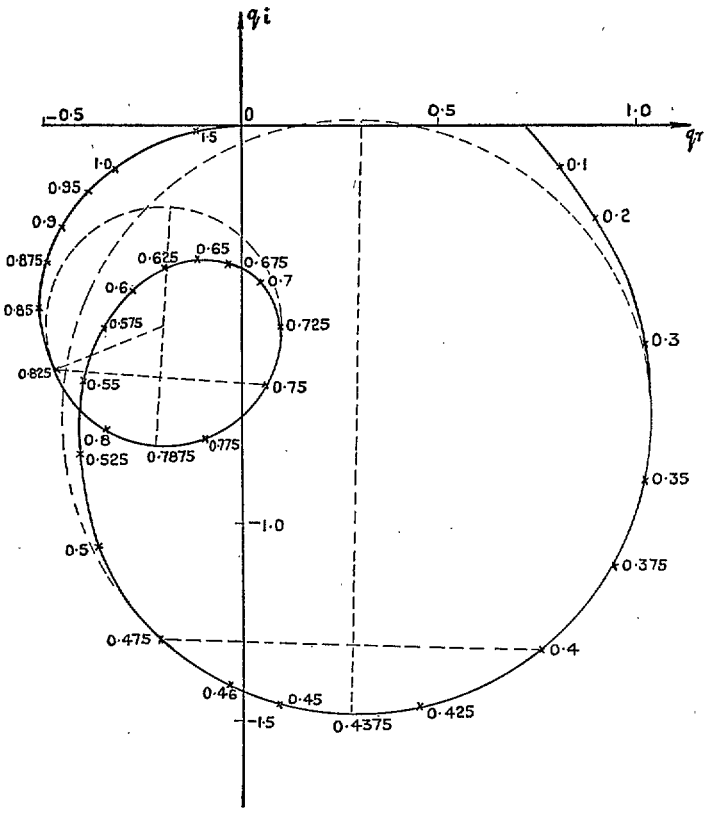

FIG. 17. Vector diagram for binary example: $v = 0{\cdot}75$, displacement 3.

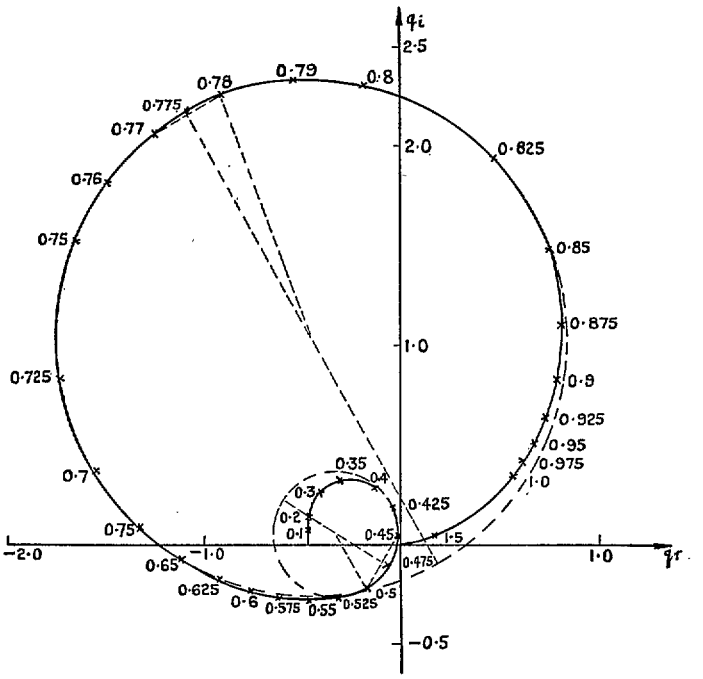

FIG. 18. Vector diagram for binary example: $v = 0{\cdot}75$, displacement 4.

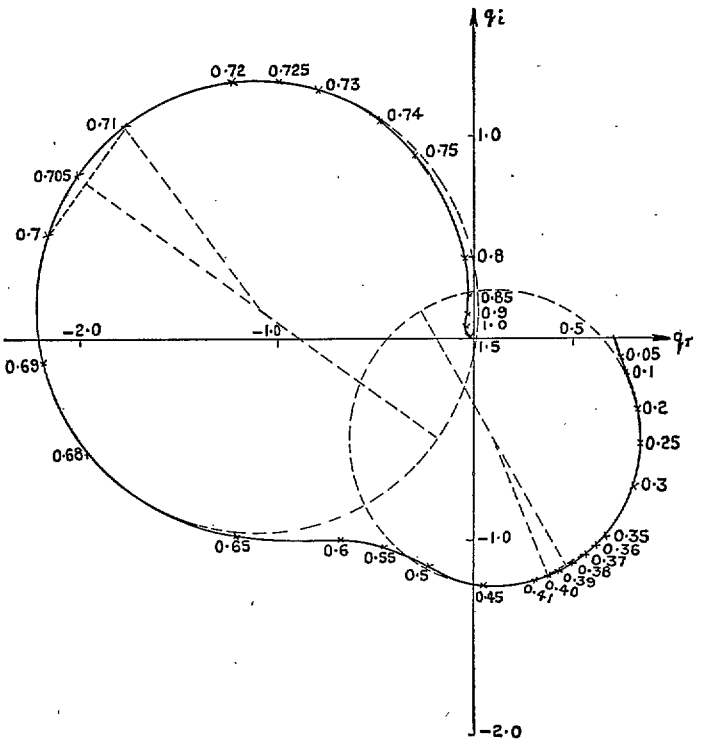

FIG. 19. Vector diagram for binary example: $v = 0{\cdot}9$, displacement 1.

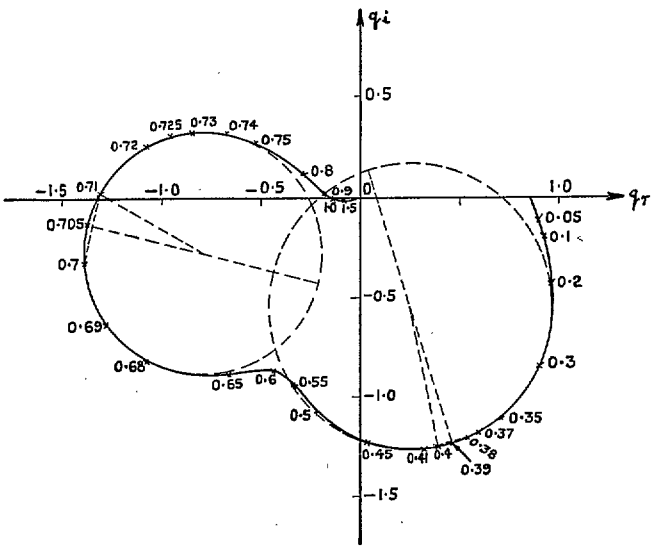

FIG. 20. Vector diagram for binary example: $v = 0{\cdot}9$, displacement 2.

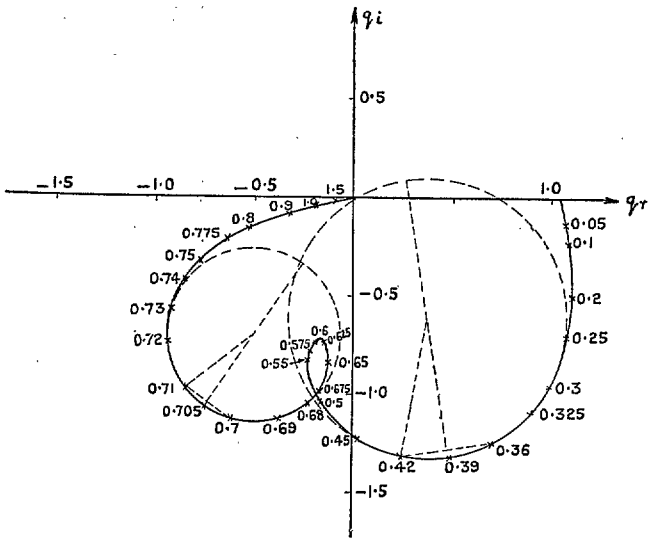

FIG. 21. Vector diagram for binary example: $v = 0{\cdot}9$, displacement 3.

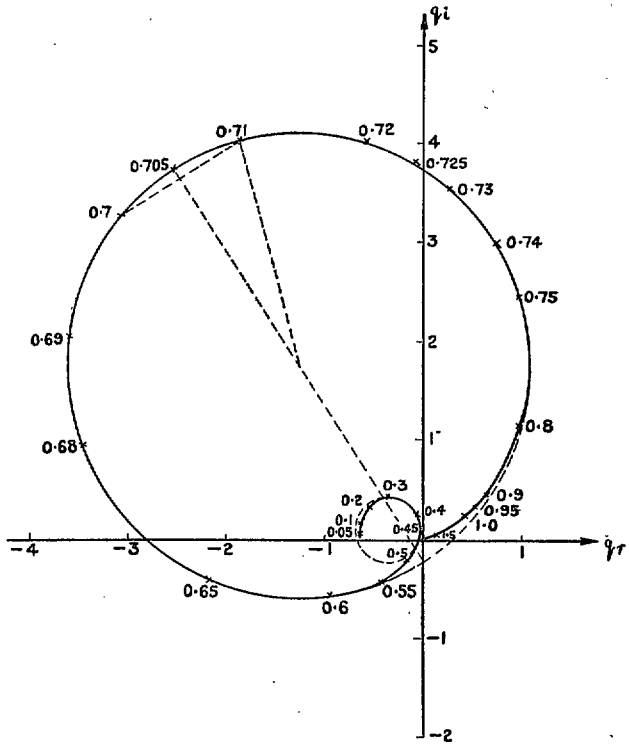

FIG. 22. Vector diagram for binary example: $v = 0{\cdot}9$, displacement 4.

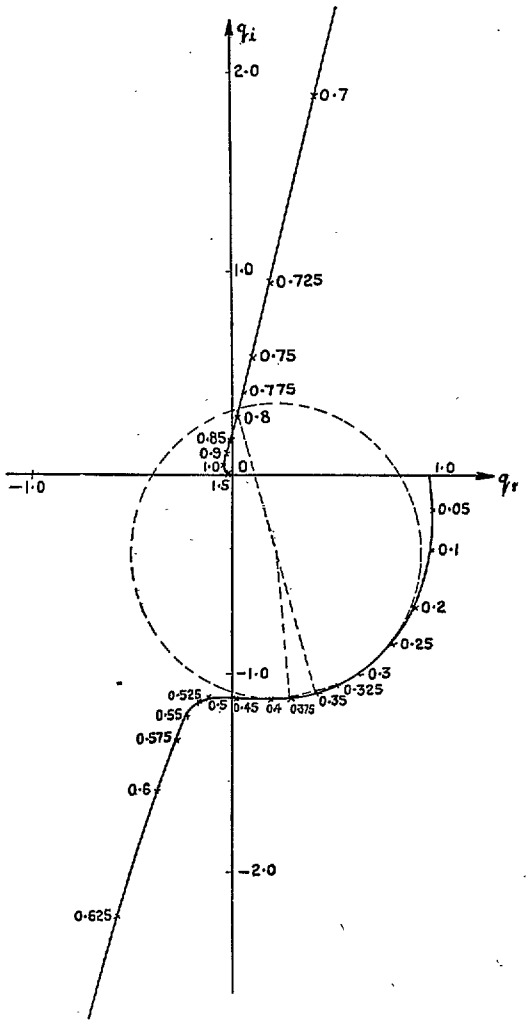

FIG. 23. Vector diagram for binary example: $v = 1{\cdot}0$, displacement 1.

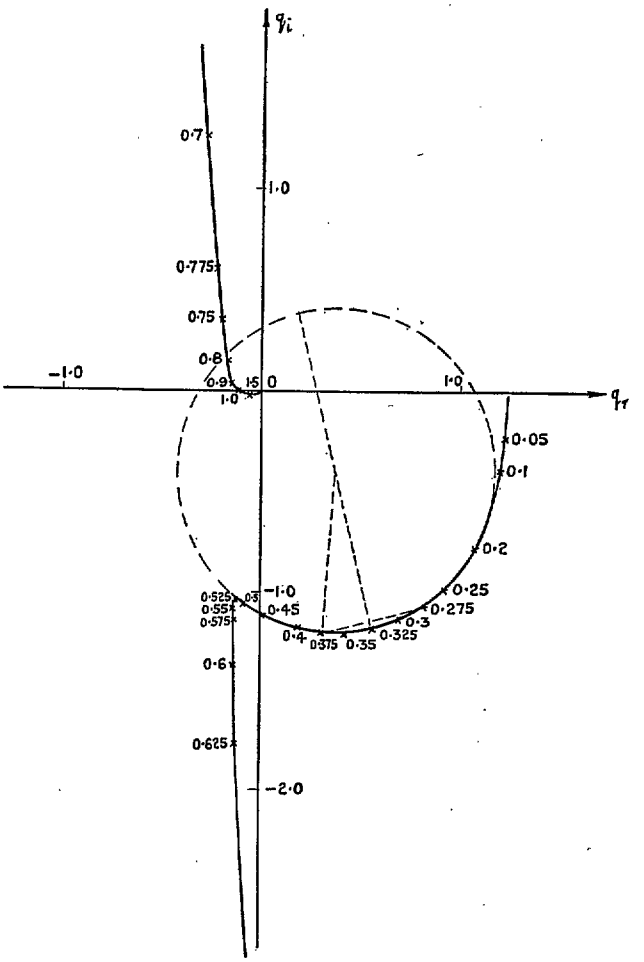

FIG. 24. Vector diagram for binary example: $v = 1{\cdot}0$, displacement 2.

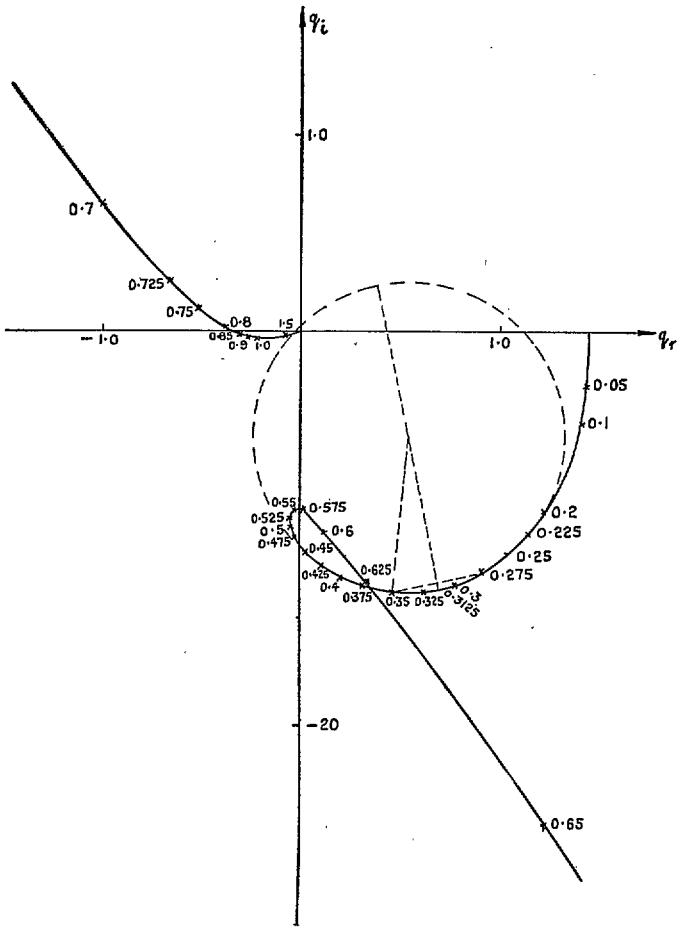

FIG. 25. Vector diagram for binary example: $v = 1{\cdot}0$, displacement 3.

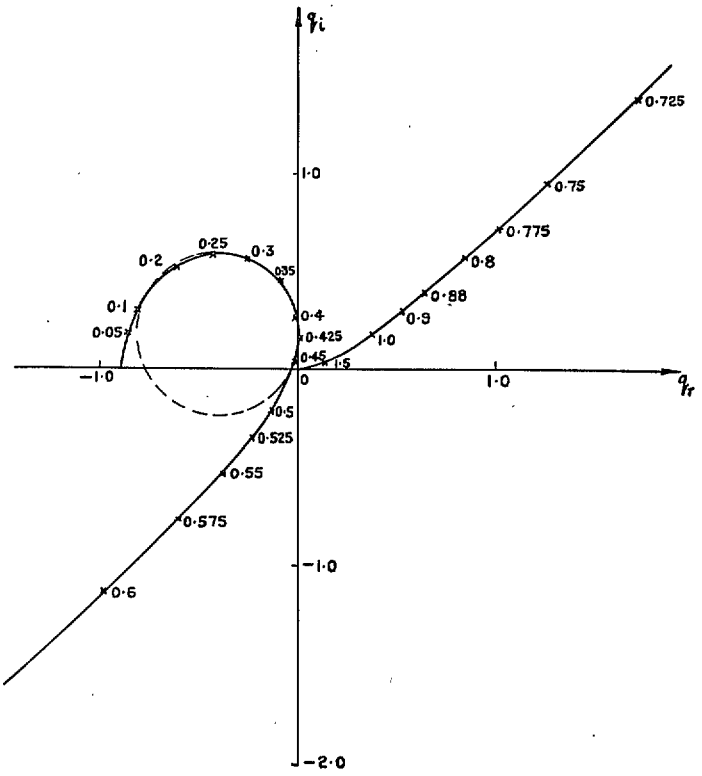

FIG. 26. Vector diagram for binary example: $v = 1{\cdot}0$, displacement 4.

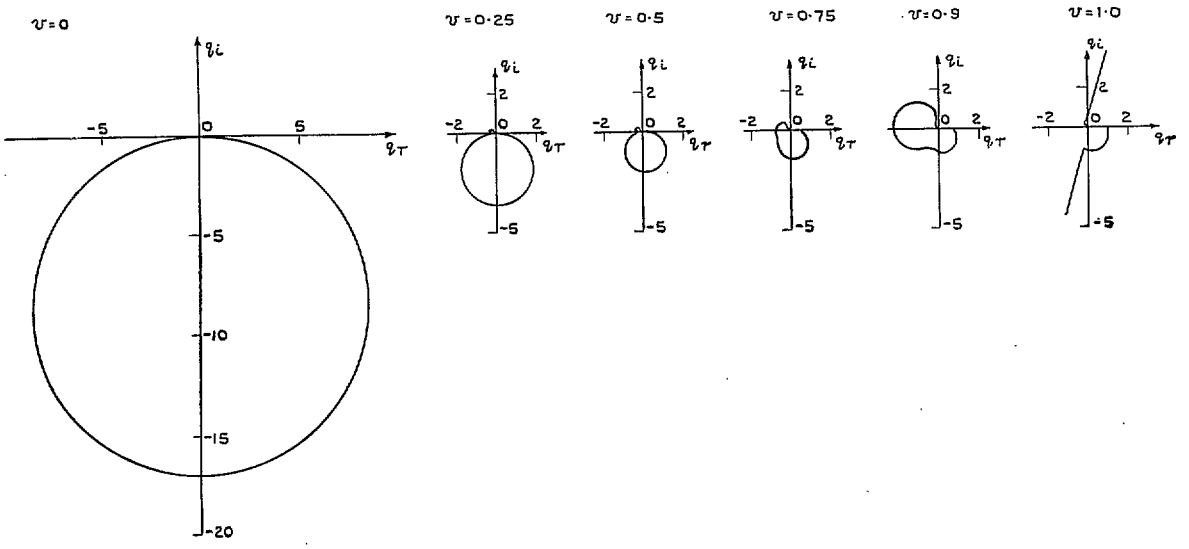

FIG. 27. Vector diagrams for binary example: displacement 1, varying speed.

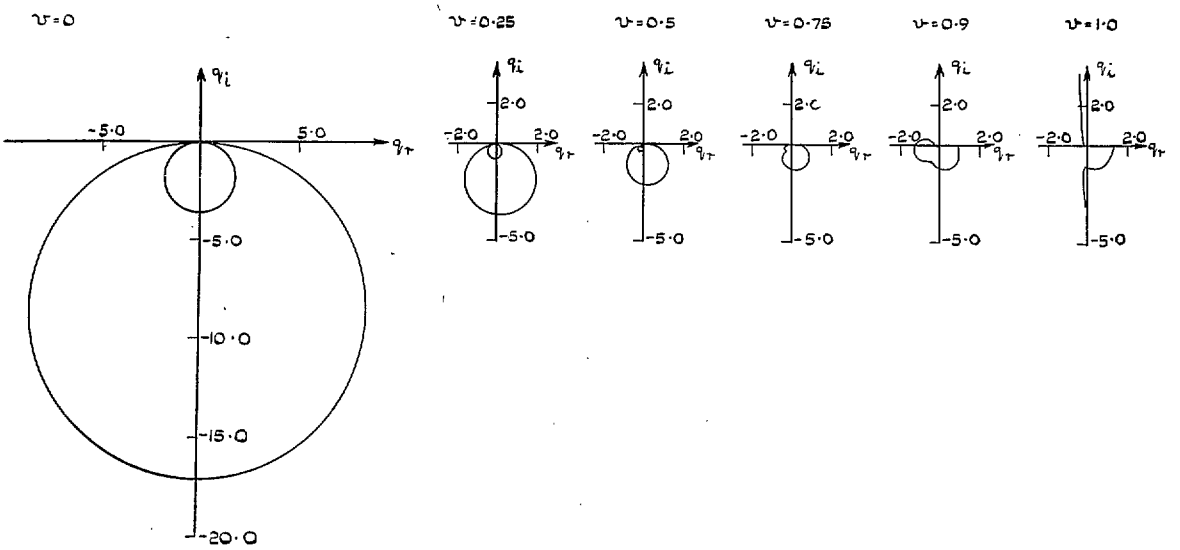

FIG. 28. Vector diagrams for binary example: displacement 2, varying speed.

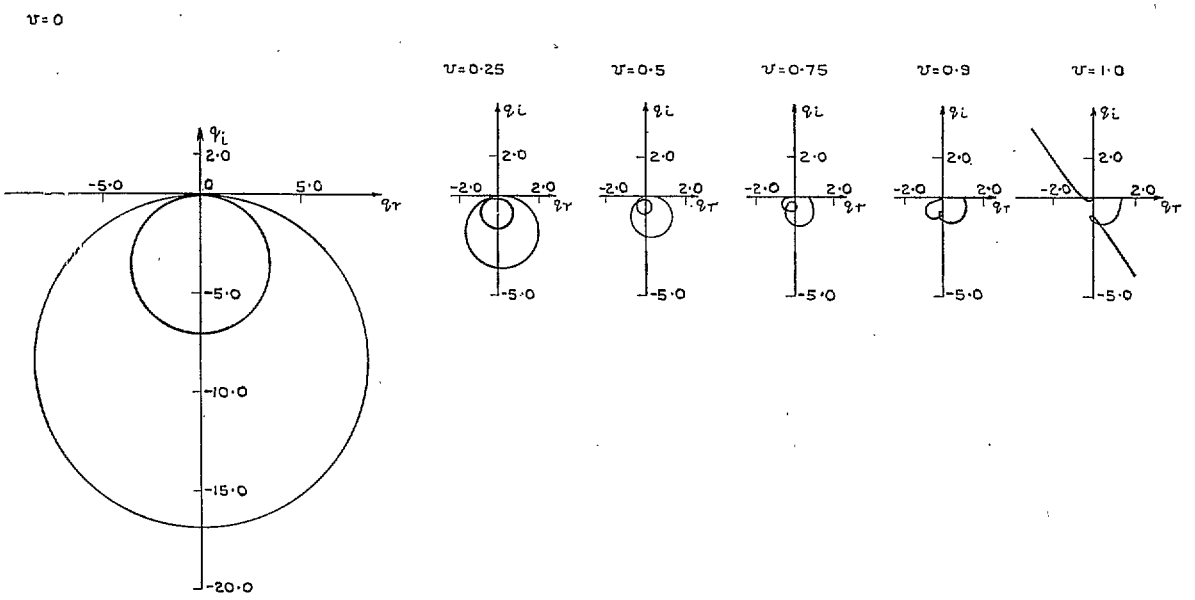

FIG. 29. Vector diagrams for binary example: displacement 3, varying speed.

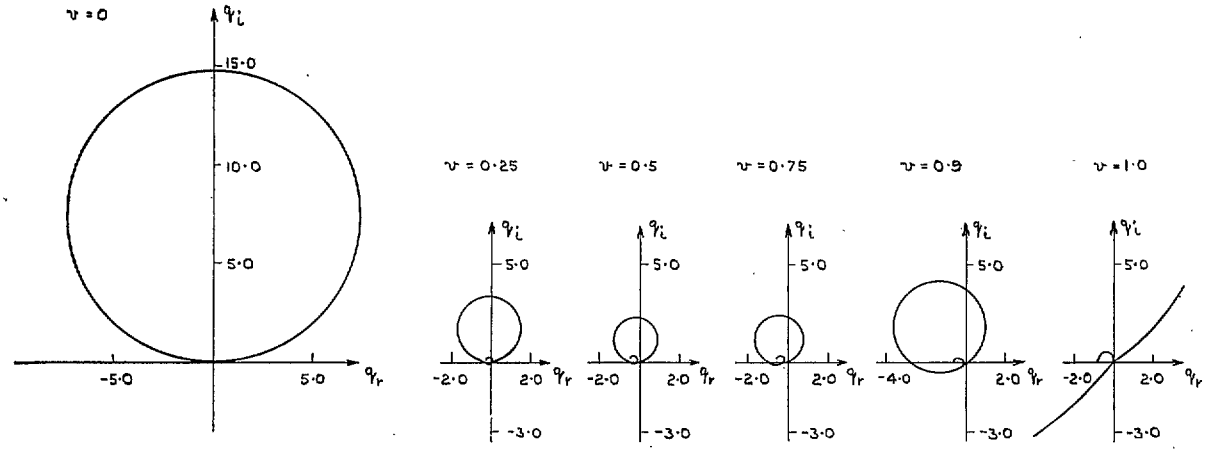

FIG. 30. Vector diagrams for binary example: displacement 4, varying speed.

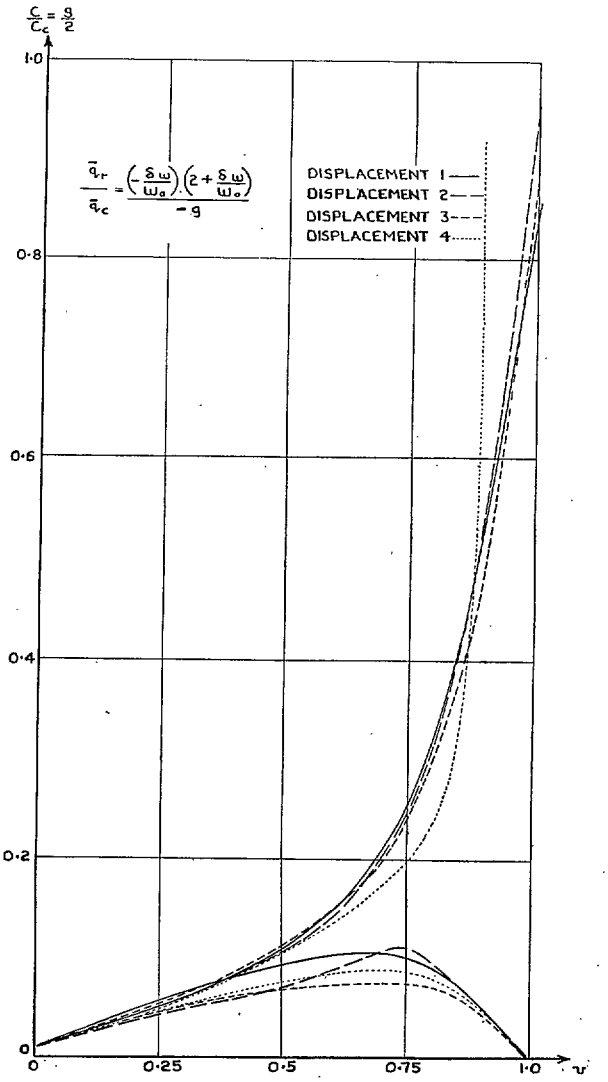

FIG. 31. Damping estimates from the vector diagrams against forward speed.

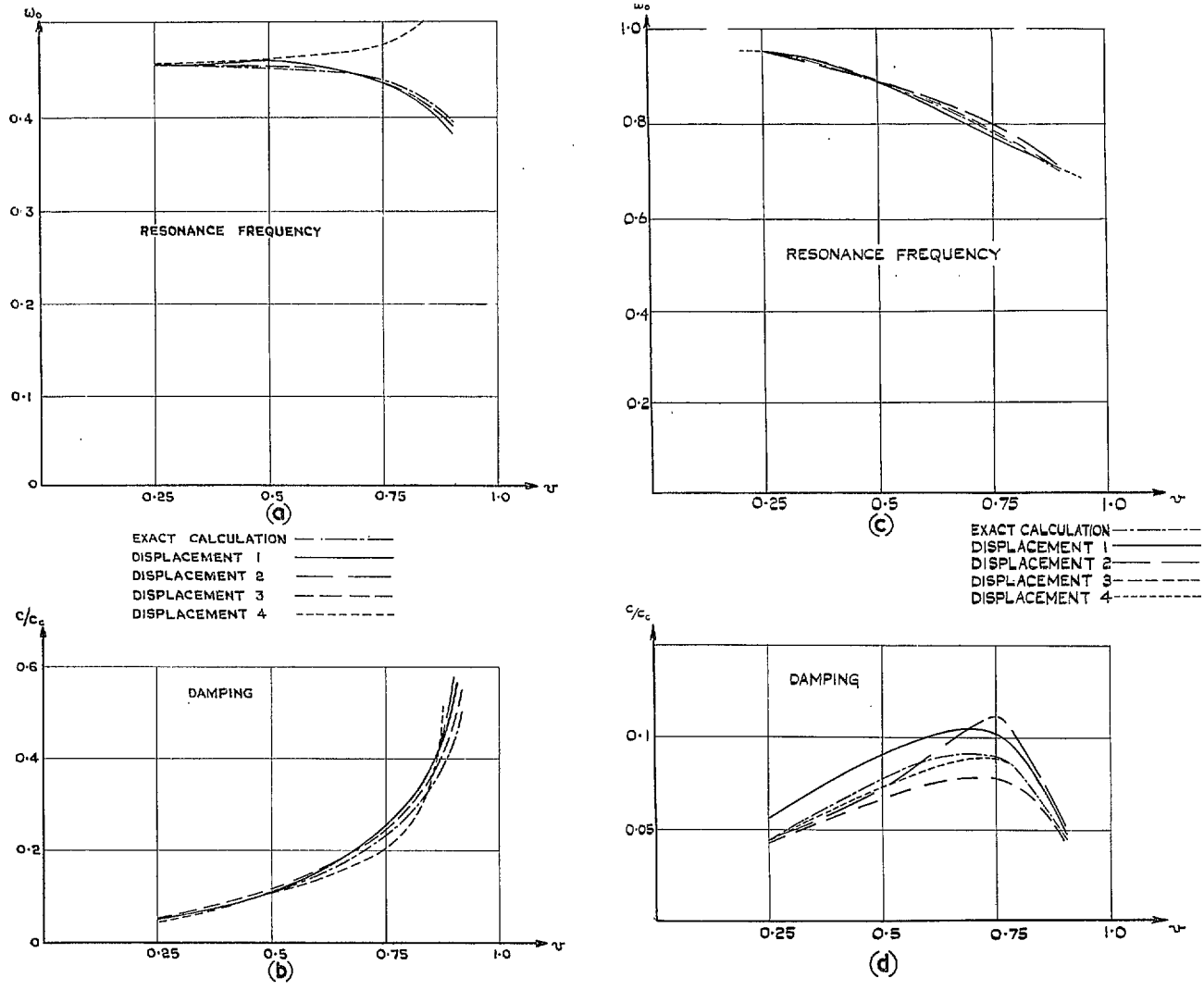

FIGS. 32a to 32d. Comparison between estimates of damping and frequency, and exact calculation.

(78800) Wt. 54/8210 K.5 2/61 Hw.

Publications of the Aeronautical Research Council

ANNUAL TECHNICAL REPORTS OF THE AERONAUTICAL RESEARCH COUNCIL (BOUND VOLUMES)

1941 Aero and Hydrodynamics, Aerofoils, Airscrews, Engines, Flutter, Stability and Control, Structures. 63*s.* (post 2*s.* 3*d.*)

1942 Vol. I. Aero and Hydrodynamics, Aerofoils, Airscrews, Engines. 75*s.* (post 2*s.* 3*d.*)
Vol. II. Noise, Parachutes, Stability and Control, Structures, Vibration, Wind Tunnels. 47*s.* 6*d.* (post 1*s.* 9*d.*)

1943 Vol. I. Aerodynamics, Aerofoils, Airscrews. 80*s.* (post 2*s.*)
Vol. II. Engines, Flutter, Materials, Parachutes, Performance, Stability and Control, Structures. 90*s.* (post 2*s.* 3*d.*)

1944 Vol. I. Aero and Hydrodynamics, Aerofoils, Aircraft, Airscrews, Controls. 84*s.* (post 2*s.* 6*d.*)
Vol. II. Flutter and Vibration, Materials, Miscellaneous, Navigation, Parachutes, Performance, Plates and Panels, Stability, Structures, Test Equipment, Wind Tunnels. 84*s.* (post 2*s.* 6*d.*)

1945 Vol. I. Aero and Hydrodynamics, Aerofoils. 130*s.* (post 3*s.*)
Vol. II. Aircraft, Airscrews, Controls. 130*s.* (post 3*s.*)
Vol. III. Flutter and Vibration, Instruments, Miscellaneous, Parachutes, Plates and Panels, Propulsion. 130*s.* (post 2*s.* 9*d.*)
Vol. IV. Stability, Structures, Wind Tunnels, Wind Tunnel Technique. 130*s.* (post 2*s.* 9*d.*)

1946 Vol. I. Accidents, Aerodynamics, Aerofoils and Hydrofoils. 168*s.* (post 3*s.* 3*d.*)
Vol. II. Airscrews, Cabin Cooling, Chemical Hazards, Controls, Flames, Flutter, Helicopters, Instruments and Instrumentation, Interference, Jets, Miscellaneous, Parachutes. 168s. (post 2*s.* 9*d.*)

1947 Vol. I. Aerodynamics, Aerofoils, Aircraft. 168*s.* (post 3*s.* 3*d.*)
Vol. II. Airscrews and Rotors, Controls, Flutter, Materials, Miscellaneous, Parachutes, Propulsion, Seaplanes, Stability, Structures, Take-off and Landing. 168*s.* (post 3*s.* 3*d.*)

Special Volumes

Vol. I. Aero and Hydrodynamics, Aerofoils, Controls, Flutter, Kites, Parachutes, Performance, Propulsion, Stability. 126*s.* (post 2*s.* 6*d.*)
Vol. II. Aero and Hydrodynamics, Aerofoils, Airscrews, Controls, Flutter, Materials, Miscellaneous, Parachutes, Propulsion, Stability, Structures. 147*s.* (post 2*s.* 6*d.*)
Vol. III. Aero and Hydrodynamics, Aerofoils, Airscrews, Controls, Flutter, Kites, Miscellaneous, Parachutes, Propulsion, Seaplanes, Stability, Structures, Test Equipment. 189*s.* (post 3*s.* 3*d.*)

Reviews of the Aeronautical Research Council

1939–48 3*s.* (post 5*d.*) 1949–54 5*s.* (post 5*d.*)

Index to all Reports and Memoranda published in the Annual Technical Reports

1909–1947 R. & M. 2600 6*s.* (post 2*d.*)

Indexes to the Reports and Memoranda of the Aeronautical Research Council

Between Nos. 2351–2449	R. & M. No. 2450 2*s.* (post 2*d.*)
Between Nos. 2451–2549	R. & M. No. 2550 2*s.* 6*d.* (post 2*d.*)
Between Nos. 2551–2649	R. & M. No. 2650 2*s.* 6*d.* (post 2*d.*)
Between Nos. 2651–2749	R. & M. No. 2750 2*s.* 6*d.* (post 2*d.*)
Between Nos. 2751–2849	R. & M. No. 2850 2*s.* 6*d.* (post 2*d.*)
Between Nos. 2851–2949	R. & M. No. 2950 3*s.* (post 2*d.*)

HER MAJESTY'S STATIONERY OFFICE

from the addresses overleaf

Printed and published by
HER MAJESTY'S STATIONERY OFFICE

To be purchased from
York House, Kingsway, London W.C.2
423 Oxford Street, London W.1
13A Castle Street, Edinburgh 2
109 St. Mary Street, Cardiff
39 King Street, Manchester 2
50 Fairfax Street, Bristol 1
2 Edmund Street, Birmingham 3
80 Chichester Street, Belfast 1
or through any bookseller

Printed in England

R. & M. No. 3125

S.O. Code No. 23-3125